International Journal of Engineering Research and Development
e-ISSN: 2278-067X, p-ISSN: 2278-800X, www.ijerd.com
Volume 12, Issue 12 (December 2016), PP.27-35

Mixed Mode Fracture Analysis of Multiple Cracks in Flat and Curved Stiffened Panels in Aircraft Fuselage Structures

S. Suresh Kumar[1], H. Ashwin Clement[2], R. Karthik[3]
[1]*Associate Professor, Department Of Mechanical Engg, SSN College Of Engg, Kalavakkam, Chennai 603 110,*
[2,3]*UG Student, Department Of Mechanical Engg, SSN College Of Engg, Kalavakkam, Chennai 603 110,*

Abstract: Aircraft panels are primarily riveted lap joints, the structural integrity assessment of these panels are of prime importance in estimating the life of these panels until failure. In real-time aircraft panels are mainly subjected to fatigue loading induced by the pressurization cycle. Multiple-site damage (MSD) is the predominant failure mode of the longitudinal splice joint, which is characterized by assembly of small cracks which may lead to premature failure due to their combined effects. When two cracks approach one another, their stress fields influence each other and produce enhancing or shielding effect depending on the position of the cracks. In the present work, an attempt has been made to compare the mixed mode stress intensity factor (SIF) of cracks in plates under the presence of flat ad curved stiffened panel. Although many SIF solutions have been proposed already, the present work concentrates on the influence of curvature effect on mixed mode SIF of multiple cracks in a plate. Diametrically opposite surface cracks with various crack depth ratios (a/t) were considered for a typical longitudinal splice joint. Frictional contact interactions were defined between rivet-hole, rivet head-sheet, sheet-sheet and stringer-sheet interfaces in order to simulate the exact service conditions. Compared to flat panels Higher SIF is observed for curved stiffened panel due to additional bending moment. It is also observed that, the presence of stiffened panel reduces the mode I fracture of flat panel by compressing the crack surfaces whereas influence of mode I fracture is higher for curved panel due to flattening of plates. The curvature effect of curved plate minimizes the effect of mode II fracture and increases the negative out of plane shear fracture with crack depth ratios.

Keywords: multi-site damage, stress intensity factor, mixed mode fracture, uniaxial and biaxial loading, crack depth ratio, stringer, curved panel

I. INTRODUCTION

The primary role of an aircraft fuselage structure during its life is to carry loads and provide required lift force. This is achieved by using thin-walled structures whose interior surfaces are reinforced by longitudinal and transverse strengthening members called stiffeners. The predominant method used for joining these elements together is riveting because it's simplicity and less time consumption. Riveted lap joints are being used traditionally for long time in the aerospace industry. These joints are considered as the crucial zones that are designed under damage tolerance procedures in the civil aircraft industry. Riveted lap joints in fuselage structure can be broadly classified into longitudinal and circumferential joints. Stringers or stiffeners are joined either by riveting, bonding or spot-welding. Stringers restrain the sheets from bulging out otherwise called pillowing and is strongly dependent on type of frame such as, shear tied frame or floating frame. Shear tied frame is the one, in which the stringer is directly riveted to the sheets and it is commonly used in passenger aircrafts. According to the theory of thin-walled pressure vessels, hoop tension is the primary loading. Fuselage is also subjected to longitudinal tension which is almost half the circumferential pressure.

Thus the longitudinal joints are more critical than the circumferential joints. Longitudinal splice joints can additionally experience bending or shear stresses resulting from air turbulence (predominantly during climb and descent period at low altitudes) and maneuvers (take-off and landing) depending upon the circumferential location of the splice and position along the fuselage. Due to the cabin pressurization, membrane stresses are generated on the fuselage skin, total effect of the pressurization is a combination of hoop and longitudinal tension. Multi-site damage (MSD) is the pre-eminent failure mode of a longitudinal splice joint due to the fatigue load induced by cabin pressurization cycle. MSD in aging aircraft is mainly due to clamping force deterioration which results from corrosion or fretting under cyclic loading and excessive out of plane deformations during service operations [4]. The significance of MSD in structural integrity of fuselage was realized immediately after the Aloha and Japan Airlines crash incidents. MSD is an important concern in aging aircraft, and deals with determining failure conditions for multiple crack configurations. Compared to single-site damage (SSD), MSD reduces the life expectancy of a joint by 30%. Figures 1 and 2 show the schematic arrangement of curved stiffened and flat stiffened panels used in aircraft fuselage portion. Three cracks are introduced at the middle row of rivets as shown in figure.2

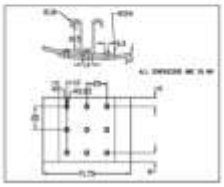

Fig 1. Schematic arrangement of curved stiffened panel

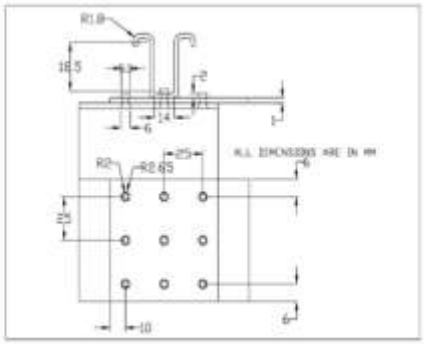

Fig 2. Schematic arrangement of flat stiffened panel

Thus, determination of fatigue life of the joint is the primary concern in designing the joint. Prediction of the life of the joint involves three phases: life until crack initiation, stable fatigue crack growth and unstable rapid MSD growth to failure. Experimental studies have shown that, a visible crack develops only after 75% of the fatigue life and thus making it possible to detect cracks through scheduled inspection. Although once visual crack has appeared, it becomes necessary to predict the residual life of the joint and hence decide the number of safe cycles for the aircraft. The structural integrity of the riveted joint with multiple cracks depends on the length of each crack, its orientation with respect to the other and the distance between cracks and the severity of stresses at the crack tips. These crack tip stresses are defined by Stress Intensity Factor (SIF). The SIF solutions obtained could be useful for correlating fatigue crack growth rates. Also they can be used to compute fracture toughness of riveted joints which have surface cracks at the plate.

. The main objective of the present work is

- Determination of mixed mode stress intensity factor (SIF) of longitudinal splice joint with multiple cracks.
- To understand the effect of curvature on SIF of multiple cracks for various crack depth (a/t) ratios.
- To understand the influence of loading conditions (uniaxial and biaxial) for various crack depth (a/t) ratios in SIF.
- To investigate the effect of friction for various (a/t) ratios in SIF.

In the present work, fracture analysis for a typical longitudinal splice joint of B737-200 with multiple cracks is done. The splice along the fuselage neutral line is chosen for analysis, so that only pressurization stresses act on the joint. SIF has been evaluated at the crack tips for (a/t) ratios ranging from 2 to 5. Through cracks of larger length are considered for analysis because most of crack growth prediction experiments done by LEFM (Linear Elastic Fracture Mechanics) approach on small cracks led to the conclusion that behavior of small cracks are anomalous and thus the results are not reliable. Literature studies also clearly suggested that once through cracks have been established, crack growth is stabilized. A comparison is also made between uniaxial loading (hoop tension only) and 'in-phase' biaxial loading (hoop and longitudinal tension). The top and front views of the FE models are shown in figures 3 and 4.

- **Finite Element Model**

The longitudinal splice joint was modeled and analyzed in ABAQUS Explicit solver. A 3-D model was drawn with dimensions of each sheet being 90mm x 70mm for flat and 90mm x 95mm for curved panel and a stringer of dimensions shown in Fig 2 is modeled. 100^{o} Flush rivets are modeled with a shank diameter of 4mm and a total of 9 rivets are assembled to the sheets in a 3x3 matrix for flat panel and 12 rivets in 3x4 matrix for curved panels. The sheets to be riveted have 9 and 12 holes each for flat and curved respectively. The outer sheet is provided with 100^{o} countersunk recess to support the rivet. Three holes are also cut in stringer, so that they can be attached to the middle row of the model. Countersunk recess is provided in the outer sheet up to $3/4^{th}$of its sheet thickness to avoid knife-edge effect. The rivets are then assembled in the respective holes in the sheets along with stringer. The assembled 3-D model is shown in the Fig 3 and 4 below.

Fig 3. 3D FE model of flat stiffened panel

Fig 4. 3D FE model of curved stiffened panel

Material properties of different grade aluminium were considered for the sheets, stringer and rivets and their properties are mention in Table 1.Through cracks of same crack length (a) are introduced on the either side of the rivet holes such that the crack plane is normal to the applied hoop tension. Four different models with differing crack depth ratios (a/t = 2, 3, 4, 5) were modeled separately and analyzed. Boundary conditions were chosen so that they simulate real-time conditions and were applied to facilitate mixed mode fracture.

Table.1: Mechanical properties of metals

S.No	Part	Material	Young's modulus(GPa)	Poisson's ratio	Yield stress (MPa)
1	Sheets	Aluminium (2024-T3 Alclad)	73	0.33	276
2	Rivet	Aluminium (2117 T4)	71	0.33	165
3	Stringer	Aluminium (7075-T6 Clad)	71.7	0.33	482

Surface to surface contact interaction is given between the following interfaces: (i) rivet hole-rivet, (ii) rivet head-sheet, (iii) sheet-sheet, (iv) stringer-sheet. Frictional contact is defined between these interfaces with a friction co-efficient (f = 0.1) because friction transmits major part of the load and leads to MSD. There is no interference or clearance between the rivet hole and the rivet. Cracks were introduced on the either side of each rivet for the middle row initiating from the rivet hole such that they are present in all 3 layers. All cracks have the same crack length (a=1.8mm, 2.7mm, 3.6mm, 4.5mm for ratios a/t = 2, 3, 4, 5 respectively) and partitions are made to define the crack front and crack seam. The region around the crack front was partitioned into 5 circular contours to provide fine mesh around the crack border and thus facilitate more accurate results. The cracks in the middle row are shown with the circular contours in the Fig 5 below. Meshed 3-D models are shown in the Fig 7 and 8. 20 node quadratic brick elements are used to get higher accuracy of results because linear elements showed convergence problems. Fine mesh was provided near the middle row and the contact regions for facilitating better convergence. Very fine mesh is provided near the crack tip regions and wedge elements are used to get better results as shown in Fig 6.

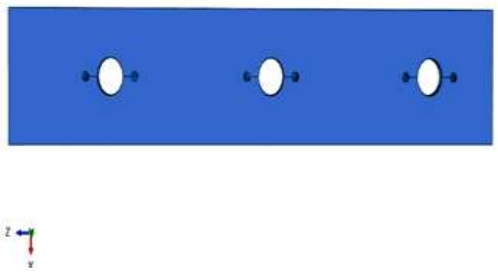

Fig 5. Cracks in the middle row of FE model

Fig 6. Meshed crack tip region

Two loading conditions have been simulated (uniaxial and biaxial) and the results are compared.

For the sake of comparison, the loads considered for flat stiffened panel are same as those for curved stiffened panel. The stringer is arrested on both the sides to inhibit its rotation.

- **Contour Integral Evaluation**

In the present work, the "Contour integral evaluation" approach was used to estimate the SIF values around the crack region. To simulate the theoretical inverse square root singularity of stresses and strains near the crack border region, singular elements were arranged around the crack border. If all the midface nodes of the 20 nodequadratic brick elements are moved to their quarter points closest to the crack line, the variations in the local stress and strain fields can be minimised. Due to 3-D nature of the crack advancement, crack propagation direction cannot be predicted and hence 'crack plane normal' approach was used to define the crack propagation direction.

- **Determination of Mixed Mode SIF**

When the riveted joint is mechanically loaded, the cracks may simultaneously open and slide relative to each other. The mixed mode fracture is formed in a joint due to complex loading condition or crack location. When the load reaches a critical value, the crack starts to grow and usually kinks into a new direction. The different modes of fracture for a growing crack are mode-I, mode-II and mode-III. In mode-I fracture the crack surfaces separate directly apart from each other and therefore it is designated as opening mode fracture. Mode II fracture causes the crack surfaces to slide over one another perpendicular to the leading edge of the crack and designated as edge sliding mode. In mode-III fracture the crack surfaces slide with respect to each other parallel to the leading edge of the crack and therefore designated as tearing mode.

In the present work, mixed mode SIF is calculated for opposite cracks located in a riveted joint using FEM. Far field tensile load is applied to the joint which causes the cracks to open and SIF values are calculated along the crack front. Currently the geometric correction factor (Y) is calculated from mixed mode fracture which includes the additional effect of mode II and mode III fracture. The mixed mode SIF is calculated from the following relation.

$$K_{mix}^2 = K_I^2 + K_{II}^2 + (K_{III}^2)/(1-\nu) \qquad \text{---------- (1)}$$

Where K_I, K_{II}, K_{III} are mode I, mode II and mode III stress intensity factors. The geometry correction factor (Y) under mixed mode condition is determined from the following equation.

$$K_{mix} = Y\sigma\sqrt{\pi a} \qquad \text{---------- (2)}$$

$$Y = K_{mix}/(\sigma\sqrt{\pi a}) \qquad \text{----------(3)}$$

Where Y- geometry correction factor, a - crack length (mm), σ -far field stress (MPa).

While computing the geometric correction factor for the uniaxial loading, the hoop stress (σ_h) value is considered as the far field stress (σ). In case of biaxial loaded joints, since the load varies on both the X-axis and Y-axis, the far field stress (σ) cannot be considered directly as hoop stress (σ_h) value. Thus an effort has been made numerically on a center cracked plate, to understand the loading behavior (uni axial and bi axial) on SIF determination. The variation is plotted in Fig 10. Initially, the hoop stress (σ_h) was increased gradually for a uniaxially loaded condition and the corresponding SIF was calculated. In the case of bi axial loading, the hoop stress (σ_h= 100MPa) was kept constant and simultaneously the longitudinal stress (σ_e) was varied in gradual steps. It is noted that, the K_{mix} value remains constant irrespective of the variation in longitudinal stress which is parallel to the crack surface. This is due to the fact that, mode I fracture significantly dominates compared to other modes of fracture and thus a far field load of 100MPa was considered.

Fig 9. Behaviour of Kmixfor varying (σh) in uniaxial specimen and varying (σe) with constant ((σh) =100MPa) in biaxial specimen The fatigue crack growth rate and residual life of the joint can be calculated from Paris equation. Table 2 shows the test matrix of loading conditions considered in the present study.

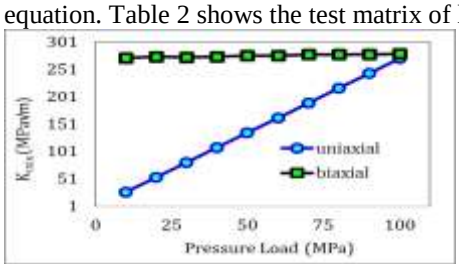

Table.2 Test matrix for numerical simulation

Structure name	Loading conditions	
	Uniaxial loading	Biaxial loading
Flat stiffened panel	a/t = 2	a/t = 2
	a/t = 3	a/t = 3
	a/t = 4	a/t = 4
	a/t = 5	a/t = 5
Curved stiffened panel	a/t = 2	a/t = 2
	a/t = 3	a/t = 3
	a/t = 4	a/t = 4
	a/t = 5	a/t = 5

II. RESULT AND DISCUSSION

SIF of multiple cracks in a riveted lap joint was calculated numerically for two different loading conditions (uniaxial and biaxial). This chapter presents the influence of crack depth ratio, loading condition and curvature on mixed mode SIF.

$$(\sigma_h) = PR/t \qquad \text{---------- (4)}$$

4.1 Load Calculation

In uniaxial loading only the hoop tension is considered. The hoop stress can be calculated by the formula

Using R= 3.23m, t= 1.6mm and altitude of 45,000sqft yields 120MPa. According to Niu (1999), it varies between 80 and 120MPa. Thus 100MPa is chosen.

In biaxial loading both hoop tension and longitudinal tension is considered. For stiffened panel, the biaxiality ratio is chosen to be 0.5 and thus longitudinal stress = 50MPa is chosen.

4.2 Effect of crack depth ratio on SIF of flat stiffened panel

Figures 10 and 11 show the effect of crack depth ratio on SIF of multiple cracks in a stiffened flat plate subjected to uni-axial (Fig.10) and biaxial loading (Fig.11) conditions. As the crack depth ratio increases, SIF increases considerably. All the three cracks (fig. 10a, 10b and 10c) shows a significant variation of SIF due to their location and load experienced by them. Since the middle region corresponds to the interface between plates, a crossover in SIF trend is observed. Similar to uniaxial loading condition, SIF values under biaxial loading are higher at the crack surface region at lower crack depths whereas at higher crack depths SIF is higher at the crack middle region. Thus one can expect higher crack growth at the plate 1 compared to stiffened panel and plate 2 region. It is also noted that the variation of SIF for uniaxial and biaxial loading conditions are marginal. A non-symmetric distribution of SIF indicates a higher crack growth rate at the plate 2 region compared to plate 1 and stiffened plate.

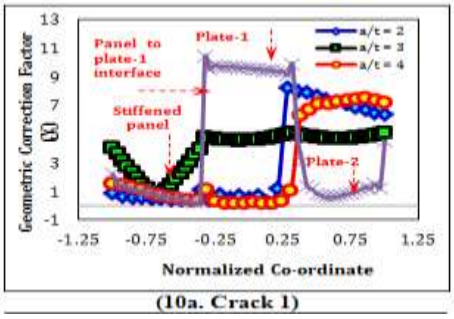

(10a. Crack 1)

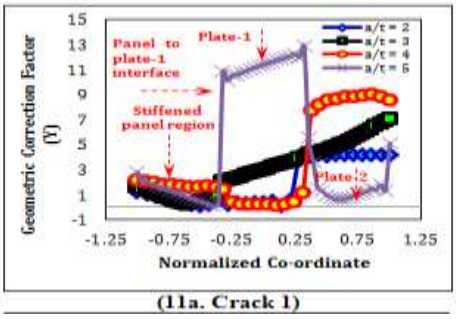

(11a. Crack 1)

4.3 Effect of crack depth ratio on SIF of curved stiffened panel

Figures 12 and 13 show the SIF variation of multiple cracks in a curved stiffened curved plate subjected to uniaxial (Fig.12) and bi-axial (Fig.13) loading conditions for various crack depth ratios. Compared to the results of flat stiffened panel, higher SIF was noticed due to additional bending moment caused by the plate curvature. Higher SIF was noticed at the crack middle region [$(S/S_0) = 0$] irrespective of the crack depth ratios. This is in contrast with the observations of flat stiffened plates where higher SIF was observed at the crack surface region [$(S/S_0) = \pm 1$] at lower crack depths. Thus one can expect earlier failure of curved panels compared to flat stiffened panels. In this condition also marginal influence of loading condition was observed.

4.4 Effect of crack depth ratio along the crack border of flat stiffened panel

Figures 14 and 15 show the effect of crack depth ratio on SIF of cracks measured along the crack border for uniaxial (Fig.14) and bi-axial (Fig.15) loading conditions. It is noted that, SIF values are not uniform with increase of crack depth ratio. Non symmetric values are observed along the crack border. Compared to

crack surface region, SIF values are higher for regions [(S/S_0) = -0.333 to +0.333] due to the contact interaction between the plates. Due to higher material resistance, SIF values are observed to be minimum at crack surface region [(S/S_0) = ±1]. Thus one can expect a cross over in SIF values for a crack depth ratio ranging between 3 to 4 at [(S/S_0) = 0.3 to 1.0]

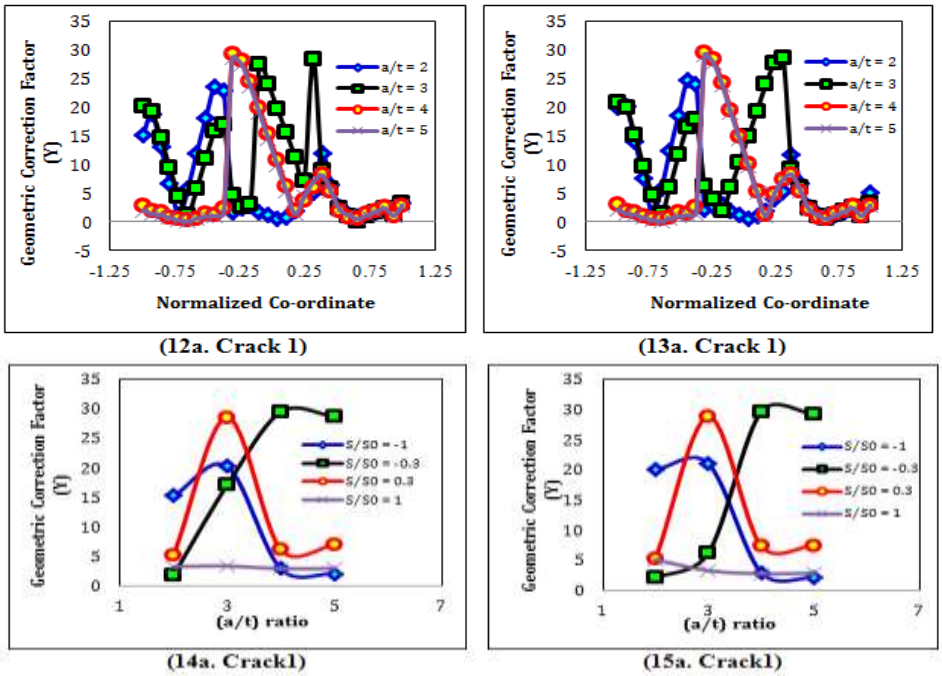

Fig 14. Effect of crack depth ratio along the crack border in flat stiffened panel – uniaxial loading
Fig 15. Effect of crack depth ratio along the crack border in flat stiffened panel – Biaxial loading

4.5 Effect of crack depth ratio on Mode I SIF of cracks in a flat stiffened panel

Plots 16 and 17 show the effect of crack depth ratio on mode-I SIF of multiple cracks in a riveted lap joint with the presence of stiffened panel under uniaxial (Fig. 16) and biaxial loading (Fig. 17) conditions. At lower crack depths, [(a/t) = 2 to 3] crack compression is observed at regions closer to the stiffened panel and mode I fracture is dominant at the other end of the crack front. The presence of stiffener causes the crack surfaces to compress at regions closer to [$S/S_0 = \pm 0.33$]. It is observed to be that, at higher crack depths, the mode I fracture plays an important role. Since the cracks 2 and 3 are opposite to each other, similar trend is noted. In contrast to uni axial loading, mode I fracture is dominant irrespective of the crack depth ratios under bi-axial loading (fig. 17). Thus one can expect accelerated crack opening mode of failure for mode I fracture under bi-axial loading condition.

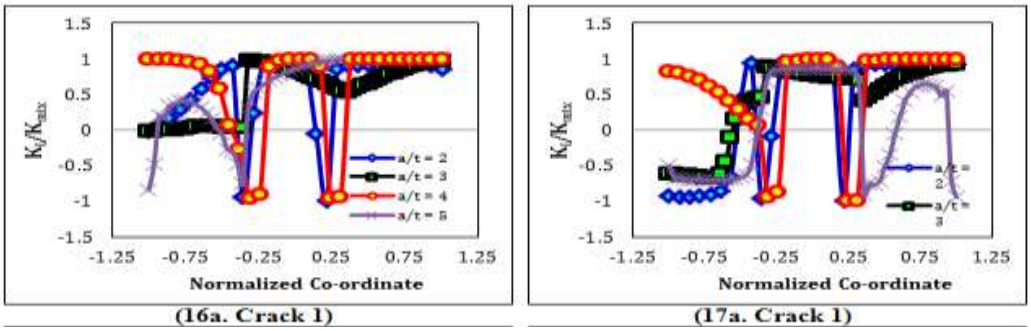

Fig. 16 Effect of Mode I fracture in flat stiffened panel– uniaxial loading condition
Fig. 17 Effect of Mode I fracture in flat stiffened panel – biaxial loading

4.6 Effect of crack depth ratio on Mode I SIF of curved stiffened panel

Figures 18 and 19 show the effect of crack depth ratio on mode-I fracture of multiple cracks in a curved stiffened panel subjected to uniaxial loading (fig. 18) and biaxial loading (fig.19). Flattening of the plate causes compression of crack surface which is reflected in fig.18. Effect of crack depth ratio was observed to be significant at lower crack depths and at surface regions. The dominant mode of fracture was observed to be mode I fracture which is in contrast to the observations of flat stiffened panel. In the case of flat panels, major failure mechanism of plates are due to crack opening mode as the load is directly used to cause the failure

whereas, equal amount of crack opening and closing mechanism is observed with the presence of curved stiffened panel which tried to flatten when subjected to external loading condition.

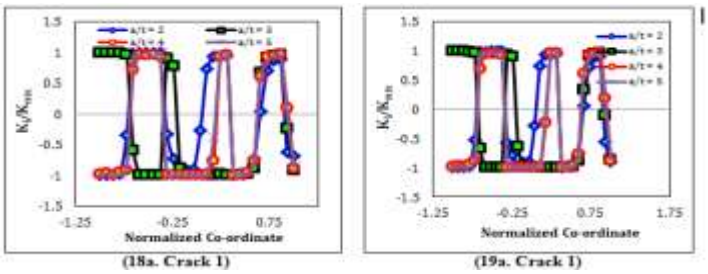

(18a. Crack 1) (19a. Crack 1)

4.7 Effect of crack depth ratio on Mode II fracture of cracks in a flat stiffened plate

Influence of crack depth ratio on mode II SIF of multiple cracks in stiffened plates is presented (fig.20). Compared to unstiffened model, non-symmetric and non-uniform SIF distribution is observed. It is observed that, at lower crack depths [(a/t) ≤ 3] the influence of mode II fracture is maximum at regions closer to stiffened panel and minimum higher crack depths [(a/t) ≥ 3]. The presence of stiffened panel minimizes the crack opening mode of failure and enhances in plane shear failure. A significant cross over in SIF distribution is observed which is due to friction between the panel and plate region. Within the plate, mode II fracture shows a uniform trend (fig.19a). As the crack depth ratio increases, mode II effect reduces gradually at the surface region which may be simultaneous increase of mode I fracture. In the case of biaxial loading, mode II effect raises within the plate region (fig.20) compared to uniaxial loading. The cross-over of SIF at the contact regions is observed to be smooth compared to uniaxial loading.

4.8 Effect of crack depth ratio on Mode II fracture of cracks in a curved stiffened panel

Influence of crack depth ratio on mode II fracture is shown in fig.22. Compared to flat stiffened panel, lesser value of SIF is observed due to curvature effect of the plate. As the crack depth ratio increases, mode II fracture observed to be decreased on one side of the crack front [(S/S_0) = -1 to 0] and increases on another side of the crack front [(S/S_0) = 0 to +1]. Thus one can expect both positive and negative in plane shear fracture in the same crack front. At middle region of the crack front [(S/S_0) = 0] marginal influence of mode II fracture was noted. Due to interaction effect, the influence of crack depth is less for crack 2 compared to crack 1 and crack3.

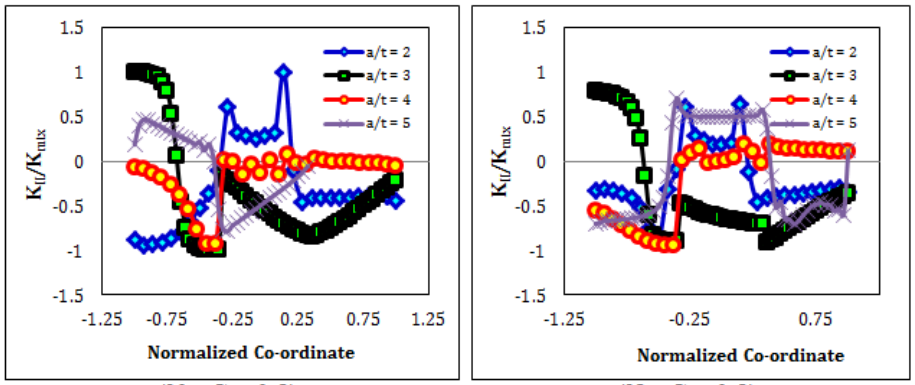

(20a. Crack 1) (21a. Crack 1)

Fig. 20 Effect of Mode II fracture in flat stiffened panel – uniaxial loading condition
Fig. 21 Effect of Mode II fracture in flat stiffened panel – biaxial loading condition

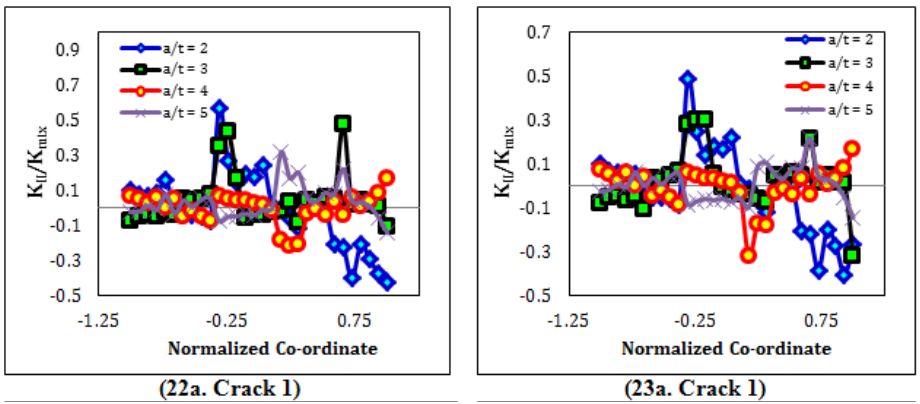

(22a. Crack 1) (23a. Crack 1)

Fig. 22 Effect of Mode II fracture in curved stiffened panel – uniaxial loading condition
Fig. 23 Effect of Mode II fracture in curved stiffened panel – biaxial loading condition

4.9 Effect of crack depth ratio on Mode III fracture of flat stiffened panel

Figures 24 and 25 show the effect of mode III SIF of multiple cracks in riveted joints under the presence of stiffener. In this geometry also, effect of mode III fracture is marginal at the crack surface region and it is more pronounced at regions closer to the middle and surface region. The abrupt change in trend is mainly due to the effect of friction between the contact regions. The non-symmetric distribution of SIF confirms the non-symmetric load distribution caused by the presence of stiffener. It is also noted that, as the distance from top surface to bottom surface increases [$S/S_0 = \pm 1$] , the effect of mode III fracture reduces which may be due to simultaneous increment of mode I and mode II fracture. Higher influence of loading is observed at higher crack depths.

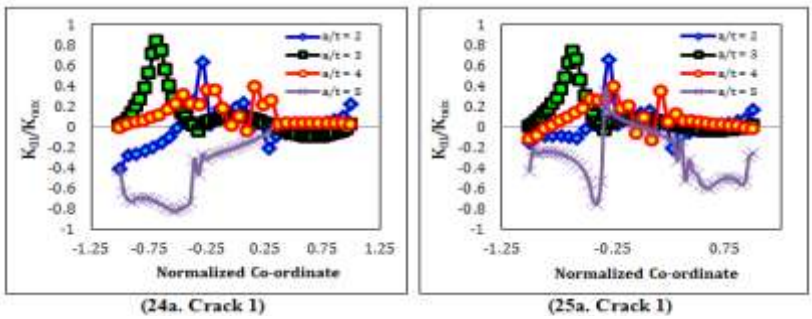

(24a. Crack 1) (25a. Crack 1)

Fig. 24 Effect of Mode III SIF in flat stiffened panel – uniaxial loading condition
Fig. 25 Effect of Mode III SIF in flat stiffened panel – biaxial loading condition

4.10 Effect of crack depth ratio on Mode III fracture of curved stiffened panel

Figures 26 and 27 show the effect of crack depth ratio on mode III fracture on SIF of multiple cracks in riveted joints with the presence of curved stiffened plates. Compared to flat stiffened plates, higher influence of crack depth ratio was observed along the crack border. As the crack depth ratio increases, the effect of mode III fracture decreases considerably along the crack border. Negative out of plane shear fracture is observed for majority of crack depth ratios considered in the present study. The effect of curved panel is to enhance the out of plane shear fracture compared to flat stiffened panel. It is also noted that, transition of positive to negative out of plane shear fracture occurs at the middle region of the crack front. Similar variation is observed for cracks 1 and 3 and the observations of crack 2 are different as the effect of crack depth ratio is suppressed by the presence of other two cracks. As the crack depth ratio increases, positive out of plane shear fracture is observed to be majority. Thus one cannot neglect of crack interaction effect during SIF determination. In this condition also limited influence of biaxial loading is observed.

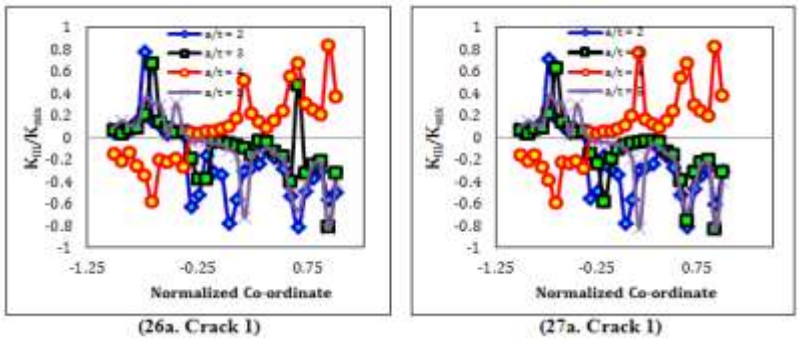

(26a. Crack 1) (27a. Crack 1)

Fig. 26 Effect of Mode III SIF in curved stiffened panel – uniaxial loading condition
Fig. 27 Effect of Mode III SIF in curved stiffened panel – biaxial loading condition

CONCLUSION

Effect of crack depth ratio on SIF (mode I, mode II and mode III) of flat and curved stiffened panel has been attempted numerically for uni axial and bi axial loading conditions. The following conclusions are made from the result and discussions.

- As the crack depth ratio increases, SIF of all the cracks increases significantly. SIF values are higher at crack surface region [$S/S_0 = \pm 1$] at lower crack depths and higher at middle region at higher crack depths. In contrast to the SIF solutions of flat stiffened panels, higher SIF was observed for curved stiffened panels Due to additional bending moment caused by plate curvature.

- The presence of flat stiffened panel causes the crack compression at regions closer to [$S/S_0 = \pm 0.33$] and mode I fracture is dominant at higher crack depth ratios [$(a/t) > 3$] under uni axial loading conditions. In contrast to the above observations, mode I fracture is dominant irrespective of the crack depth ratios in the presence of curved panel. This is mainly due to the fact that, flattening of curved panel causes additional bending moment which increases crack opening mode of failure.
- In case of flat stiffened panels, effect of in-plane shear fracture is high at lower crack depths [$(a/t) \leq 3$] and the effect reduces with increasing crack depth ratios which is due to simultaneous increment of crack opening mode fracture. In contrast to the observations of flat panel, the curvature effect of the panel minimizes the effect of mode II fracture significantly.
- The effect of mode III fracture is significant at regions closer to the crack surface [$S/S_0 = -0.33$] and increases with crack depth ratios. The effect gradually reduces along the crack border due to concurrent raise of mode I and mode II fracture. In the case of curved panels, negative out of plane shearing of plate is observed to be maximum.

REFERENCES

[1]. Muller, R.P.G., "An experimental and analytical investigation on the fatigue behavior of fuselage riveted lap joints," The significance of the rivet squeeze force and a comparison of 2024-T3 and Glare 3, Ph.D. thesis, Tu Delft, Delft (1995)

[2]. Schijve, J., "Multiple-site damage in aircraft fuselage structures," Fatigue Fract. Eng. Mater.Struct. 329-144 (1995)

[3]. Szolwinski, M.P., Harish, G., McVeigh, P.A., Farris, T.N., "The role of fretting crack nucleation in the onset of widespread fatigue damage: analysis and experiments," (1997)

[4]. Terada, H., "A proposal on damage tolerant testing for structural integrity of aging aircraft-learning from JAL accident in 1985," In Erdogan, F. (ed.) Fracture Mechanics. ASTM STP 1220, Vol.25. pp. 557-574. ASTM, Philadelphia (1995).

[5]. Vlieger, H., "Results of uniaxial and biaxial tests on riveted fuselage lap joint specimens," In Harris, Ch.E (1994).

[6]. J.J.M. de Rijck, S.A. Fawaz, "□ Stress Intensity Factor Solutions for Countersunk Holes Subjected to Combined Loading."

[7]. Lucas F.M. Silva, J.P.M. Goncalves, F.M.F. Oliveira, and P.M.S.T. de Castro. "Multiple-site damage in riveted lap-joints: experimental simulation and finite element prediction".

[8]. A. Skorupa, M. Skorupa, T.Machniewicz, A.Korbel, "Fatigue crack location and fatigue life for riveted lap joints in aircraft fuselage"

[9]. M. Skorupa, A. Skorupa, T. Machniewicz, A. Korbel., "Effect of production variables on the fatigue behaviour of riveted lap joints"

[10]. Galip Keçelioğlu, Master's thesis, Middle East Technical University, Nov 2008, "Stress and Fracture Analysis of Riveted Joints"

[11]. M. Skorupa, A. Skorupa,"Riveted lap joints in aircraft fuselage: Design, Analysis and Properties"

Nomenclature

A	crack length (mm)
T	Thickness of the sheet (mm)
S,S_0	points along the crack front
(a/t)	crack depth ratio
Y	Geometric correction factor
S/S_0	Location ratio
	Hoop stress (MPa)
	Longitudinal tension (MPa)
P	Internal pressure (MPa)
R	Radius of the fuselage (mm)
σ	Far field loading (MPa)
K_{mix}	Effective stress intensity factor (MPa√m)
f	Fricton co-efficient